

## New Ultramarine Generations from Egyptian Raw Materials

Morsy M. Abou Sekkina, Nehal A. Salahuddin, A. Elmaghraby and Mona Y. El-Ashry

Chemistry Department, Faculty of Science, Tanta University, Tanta, EGYPT

Ceramic Department, National Research center, Cairo, EGYPT.

Available online at: [www.isca.in](http://www.isca.in)

(Received 09<sup>th</sup> April 2011, revised 22<sup>nd</sup> April 2011, accepted 23<sup>rd</sup> April 2011)

### Abstract

*New ultramarine generation have been prepared by the solid state mixing and firing technique from Egyptian Raw Materials for the first time. The raw materials used includes kaoline, Na<sub>2</sub>CO<sub>3</sub>, charcoal and sulphur precursors. The action of NH<sub>4</sub>Cl on the obtained ultramarine has been studied using X-ray, UV absorption and DC-electrical conductivity, whereas a midet esr appears. Results of TGA, DTA and electrical conductivity have been undertaken and interpreted for the first time.*

97

### I. Introduction

Kowalak et al.<sup>1</sup> found that alternative methods of ultramarine synthesis involving zeolites as principal substances were developed in their lab contrary to the conventional technology. Introduction of sulfur radical precursors into the zeolites allows one to obtain ultramarine with almost negligible emission of SO<sub>2</sub> upon calcination. The polysulfides S<sub>3</sub><sup>2-</sup> and S<sub>6</sub><sup>2-</sup> seem to be the most effective precursors. Modification of hydrothermal synthesis of sodalite in the presence of sulfur compounds (including sodium thiosulfate) don't result in products of deep blue colouration. Thermal crystallization of the mixture containing kaolin and sodium polysulfides, which were carried out under the industrial conditions, resulted in the product similar to the common ultramarine.

Gobeltz et al.<sup>2</sup> investigated the encapsulation of the chromophores into the sodalite structure during the synthesis of the blue ultramarine pigment from metakaolin, sulfur, sodium carbonate and a reducing agent. The insertion of the chromophores occurs during the formation of the sodalite structure and also after its formation by diffusion into the sodalite cages. The possibility of diffusion of the chromophores into the sodalite structure was proved independently by synthesis of blue ultramarine pigments from sodalite, previously

synthesized and mixed with a source of polysulfides.

Kowalak<sup>3</sup>, investigated that ultramarine analogs are manufactured by roasting zeolites A, X, Y or sodalite impregnated with S radical (Chromophore precursors and optionally reducing agents, e.g. pitch. The precursors are S or alkali metal (preferably Na) polysulfides and the calcination is carried out preferable at 973 – 1173 K in the presence of partial absence of the air followed by reheating at 723 – 1023 K in the air for example, a little pigment was manufactured by roasting comminuted zeolite A mixture with Na<sub>2</sub>S. 9H<sub>2</sub>O Combined with pitch.

The loss of weight of the reaction mixture during calcination is < 5% and SO<sub>2</sub> emission is significantly lower than in the traditional procedures employing kaolin instead of zeolites.

Tae et al.<sup>4</sup> studied the reaction mechanism in synthesis of ultramarine blue from kaolin, S, Na<sub>2</sub>CO<sub>3</sub>, SiO<sub>2</sub> and rosin by thermal analysis, powder X-ray diffraction analysis and Ramon scattering. The mixture of the raw materials was calcined at 820<sup>o</sup>C for 5 hrs. (heating rate; 0.1<sup>o</sup>C/min) to form the ultramarine green, which was the intermediate products of the ultramarine blue. The ultramarine blue was finally prepared with the oxidation of ultramarine green at 500<sup>o</sup>C.

In the calcination process, the Na sulfides were generated by the reductive reaction of  $\text{Na}_2\text{CO}_3$ , S and rosin at  $400 - 500^\circ\text{C}$ , and the  $\text{NaAlSiO}_4$  was formed by the synthesis of anhydrous amorphous kaolin and the Na sulfides at  $\sim 600^\circ\text{C}$ , and the ultramarine green begun to form at  $\sim 700^\circ\text{C}$  with the reaction of the  $\text{NaAlSiO}_4$  and the Na sulfides. In the oxidation process, the S atoms transformed the ( $\text{S}_2^-$ ) ions of the ultramarine into ( $\text{S}_3^-$ ) ions, and these reactions caused the ultramarine green to convert the ultramarine blue. The lattice parameter of ultramarine green was increased during oxidation.

Kowalak<sup>5</sup>, showed that a reaction mixture containing kaolin, soda or other alkaline compound, an agent facilitating incorporation of anion radicals ( $\text{S}_3^-$ ) into sodalite structure, and reducing agent is roasted at 1023 K and then at  $\sim 829$  K to give ultramarine. The agent facilitating incorporation of anion radicals ( $\text{S}_3^-$ ) into sodium structure is selected from alkali metal sulfides, preferably sodium sulfide.

Leschewski and Moller<sup>6</sup>, deduced that when blue ultramarine is fused with  $\text{HCOONa}$  a white product results without loss of S. This white substance is leuco-ultramarine and is reconnected into coloured product by atmo, by removal of alkali by means of S, by treatment with Cl water of Cl gas or fusion with alkali chlorates or nitrates, blue ultramarine boiled with ethylene chlorohydrine loses most of its Na content by removal of alkali and becomes white. Fusion with NaCl does not restore the colour but fusion with  $\text{Na}_2\text{S}$  produces a delicate blue and boiling  $\text{Na}_2\text{S}$  solution gives a delicate green.

Jaeger<sup>7</sup>, showed that the ultramarines are stable toward alkalis but unstable toward acids. Na can be replaced by Li (bluish violet), Rb, Cs, K, Tl (violet), Ag (light yellow), Mg (light blue) and other bivalent metals (colourless) by treatment in aqueous solution at  $100 - 120^\circ\text{C}$ . Replacement of S by Se or Te yields blood-red or yellow ultramarine resp. They possess hydraulic properties and resemble permutites in many respects. The substitution of Na by Ag leads to an equal

dependent on concentration and temperature and that of Ag by alkali goes more readily with iodides than with chlorides. Replaceability and reaction velocity increase with decrease in at. wt. of the alkali metal. All these ultramarines yield spectrograms identical with those of nosean and hauynite. The centered cubic lattice has a 9.13 A.u. The space groupings of the atoms, certain of which appear to be "wandered" are discussed.

Hoffmann<sup>8</sup>, showed that the sodalite complex possesses an inert silicate component,  $\text{Na}_4\text{Al}_4\text{Si}_6\text{O}_{24}$  which in the presence of  $\text{Na}_2\text{SO}_3$  takes part in reaction as  $\text{Na}_6\text{Al}_4\text{Si}_6\text{O}_{24}$ . Ultramarine substrates exhibit characteristic irradiation effects corresponding to their chemical compound and these present a series of colour changes opposite in direction to those obtained with polysulfide S. Irradiation of white-green and violet ultramarine produces colour alterations which no longer occur if the return of the dissociation. S in blue ultramarine into the original complex is prevented. The behaviour of blue ultramarine is not contrary to the assumption that ultramarine is definite S atoms of the various substrates.

Kook et al.<sup>9</sup> showed that ultramarine blue was synthesized with Kaolin, sulfur, sodium carbonate, silica and rosin, and its reaction mechanism was investigated. The mixture of the raw materials was calcined at  $820^\circ\text{C}$  for 4 hrs (heating rate:  $2^\circ\text{C}/\text{min}$ ) to form the ultramarine green, which was the intermediate of ultramarine blue. The ultramarine blue was finally prepared with the oxidation of the ultramarine green at  $500^\circ\text{C}$ . The reaction products and the structural changes of ultramarines appeared in this synthesis were established by power X-ray diffraction analysis and Raman Scattering. The sodium sulfide and the  $\text{NaAlSiO}_4$  were generated at  $500^\circ\text{C}$  and  $620^\circ\text{C}$  respectively in calcination process and the ultramarine green was appeared at near  $740^\circ\text{C}$  with the reaction of sodium sulfates and  $\text{NaAlSiO}_4$ . Also, the formation of ultramarine blue was caused by the sulfur atoms generated from the oxidation of sodium sulfide which existed in ultramarine green.

Ultramarine blue pigments have been investigated by EPR and Raman spectroscopies, as well as by

colorimetry-for the first time, correlations between EPR, Raman, and colourimetric parameters of these pigments have been established. It's now established that there isn't only one blue ultramarine but different shades of blue depending on the relative concentrations of blue and the yellow chromophores. The greenish and reddish shades of blue are characterized by EPR. Raman and colourimetric parameters as suggested by N-Gobeltz et al.<sup>10</sup>.

Balkus and Kowalak<sup>11</sup> worked on the crystallization zeolites (A, X, hydroxysodalite) in the presence of sulfur compounds in order to incorporate them into the intracrystalline cavities already on nucleation of the zeolite structure. This method of encapsulation has been proved successful for various metal complex compounds.

The major goal of the present investigation is to discover new ultramarine generations from Egyptian raw materials for inorganic pigments industries.

### Materials

These above samples (kaolin, anhydrous sodium carbonate, charcoal and sulfur precursor are finely ground together and tightly packed into a small porcelain crucible which is then covered; the crucible is heated to at least a bright red for 1.5 hrs. Then the cover is removed and after firing for an additional 2 hrs and cooling, the ultramarine easily separated forms the uncoloured materials. Composition and condition of preparation of the ultramarine samples are shown in table (1).

**X-ray Diffraction analysis:** The prepared samples were subjected to Cu-K $\alpha$  X-ray analysis using Shimadzu (Japan) X-ray diffractometer, using Ni-filter at room temperature in the range  $2\theta = 10-70^\circ\text{C}$ .

**Infrared Absorption Spectral Measurements:** The room temperature IR absorption spectra were recorded using the solid KBr disk technique and a-Perkin Elmer infrared spectrophotometer in the range  $4000 - 200 \text{ cm}^{-1}$ .

**Electronic Absorption Spectral (UV/VIS) Measurements:** The ultramarine (blue and violet)

samples were subjected to UV/Visible absorption spectral measurements using the Nujol mull (glycerine suspension) solid technique and the results were compared to those of commercial ultramarine (produced by Reckit's Colours of Polifarb). A PYEUNICAM SP 800 spectrophotometer was used in the range 900 to 200 at room temperature.

**Thermogravimetric analysis (TGA):** TGA is measure of the amount and rate weight change of material, as a function of increasing temperature (weight change in temperature). Our measurements were undertaken in the temperature range  $0 - 800^\circ\text{C}$  in air using Shimadzu (Japan) Thermal Analysis.

**Differential thermal analysis (DTA):** DTA is a technique in which a record is made of the temperature difference between the sample and the reference material against time or temperature. DTA records every enthalpy, exothermic and endothermic as caused by structural or chemical changes. In the temperature range (10 mv/cm) from 20 up to 600 with pure  $\text{Al}_2\text{O}_3$  as a reference material using DT-30 Shimadzu thermal analyzer in air.

**Electronic Spin Resonance Measurements:** The Electron Spin Resonance spectra were recorded at X-band frequencies on JES-FE 2 XG, ESR spectrometer at room temperature at the Central Research Lab, Tanta University, Egypt. The magnetic field was swept from 0 to over 8 KG and the calibrated energy was 1 KG with a digital gaussmeter. Several selected samples were investigated and showed identical features. DPPH was used as internal reference.

**DC-Electrical Conductivity Measurements:** The DC-electrical conductivity was measured using the two terminals DC-method. The pellet was inserted between spring loaded copper electrodes. A Kiethely 175-Multimeter (USA) was employed from room temperatures up to 573 K. The temperature was measured by a calibrated chromel-alumel thermocouple placed firmly at the samples. Measurements were conducted in such a way that at each temperature a sufficient time was allowed for thermal equilibrium.

### Results and Discussion

Fig. 1 display the Cu-K $\alpha$  X-ray diffraction pattern of ultramarine samples. It can be easily seen that, the kaolinite phase disappeared completely from X-ray pattern of the ultramarine. This suggests the complete formation of ultramarine instead of kaolinite phase. As deduced by Stoky et al.<sup>12</sup> for both natural (Lazurite, Laps lazuh) and synthetic ultramarine show the structure of sodalite. From (ASTM card No. 3 - 0334) ultramarine sample have the formula ( $\text{Na}_4\text{Al}_3\text{Si}_3\text{O}_{12}\text{Cl}$ ) sodium aluminium silicate. As illustrated in table 1, the sulfur source affects the structure and the colour of the resulting ultramarine samples, Thus XRD pattern given in fig. 1 show that calcination with sodium polysulfides leads to sodalite structure<sup>13</sup>.

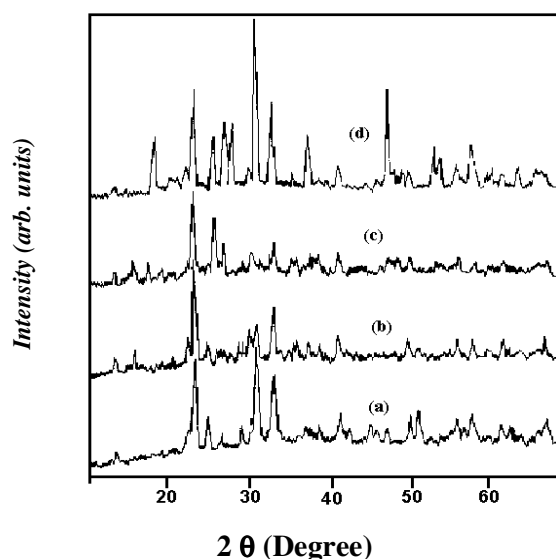


**Figure-1: The X-ray diffraction patterns of the prepared ultramarine samples containing:**  
 a. sulfur element, b.  $\text{Na}_2\text{SO}_3$ , c. sulfur and  $\text{Na}_2\text{SO}_3$ , d. sulfur and  $\text{Na}_2\text{SO}_3$  (fired for 10 hr)

In the case of elemental sulfur an unknown structure is formed where as in the case of  $\text{Na}_2\text{S}$  and  $\text{Na}_2\text{SO}_3$ , condensed phases of crystobalite is predominant<sup>14</sup>. This takes place after firing to 400°C for 2 hrs and at 750°C for hrs. But for samples (5) and (6) pure sodalite structure has been formed after firing at 750°C for 6 hrs. It's therefore seems that the sulfur compounds are responsible for directing the recrystallization, which means act as templates<sup>15</sup>, see fig. 1, table 2. The effects of sulfur precursor and firing condition

on the colour and structure of the produced ultramarines.

Since the sodalite structure with formula  $\text{Na}_4\text{Al}_3\text{Si}_3\text{O}_{12}\text{Cl}$  with cages of 0.6 nm in diameter are stable and they can host variety of molecules (e.g. NaCl in Natural sodalite). Even large molecules containing as many as seventeen atoms can be encapsulated<sup>16</sup>. So encapsulation of elemental sulfur and sulfur precursor is available.

The calcination at high temperature (~ 800°C) was usually conducted with reductive agent (Pitchtar). The resulting samples show intense blue colouration similar as natural ultramarine. The interesting structure transformation towards sodalite was noticed for impregnated zeolites A, X, Y upon heating at temperatures higher than 600°C<sup>17</sup>. X-ray patterns also display that most of peaks are characteristics to synthetic ultramarine nearly at the same positions as those of sodalite structure but may be shifted to lower  $2\theta$  i.e. increase d-spacings. This is ascribed to the encapsulation of either sulfur element or sulfur precursor in the sodalite cages. These are of larger diameter than that of chloride in natural sodalite. In natural sodalite the maximum intensity is that of peak at  $2\theta = 24.52^\circ$  but in our synthetic ultramarine samples, the maximum intensity is that of peak at  $2\theta \cong 24^\circ$  for samples (3) and (4) that containing  $\text{Na}_2\text{S}_2\text{O}_3$  and  $\text{Na}_2\text{SO}_3$  which is similar to that of natural sodalite on the other hand we found that the maximum intensity is that of peak at  $2\theta \cong 32^\circ$  for sample (5), (6) (These samples are of blue and intense blue colour. This is interpreted on the basis of formation of other ultramarine phase.

Fig. 2 shows the effect of adding  $\text{NH}_4\text{Cl}$  on the values of  $2\theta$  and ( $d \text{ \AA}$ ) of ultramarine blue (containing S and  $\text{Na}_2\text{SO}_3$ ). We found that, the maximum intense peak is that appear at  $2\theta = 28.33^\circ$  shifted to lower  $2\theta$  value in a comparison to ultramarine blue containing (sulfur element and  $\text{Na}_2\text{SO}_3$ ). Nearly all characteristic  $2\theta$  values of our synthetic ultramarine shifted to lower  $2\theta$  value (higher  $d \text{ \AA}$ ) values mean that  $\text{Cl}^-$  ions replaces  $\text{S}_3^-$  radical and thus causing fading of blue colour. It has been found that upon the addition of  $\text{NH}_4\text{Cl}$  to ultramarine sample prepared by using elemental

sulfur and  $\text{Na}_2\text{SO}_3$  as sulfur precursor we found that the blue colour undergo faddening and become violet. The maximum intense peak at  $2\theta \cong 32^\circ$  that characteristic for sodalite, shifts to lower  $2\theta$  value (increased d-spacing) whereas  $\text{S}_3^-$  radicals are responsible for blue colour.

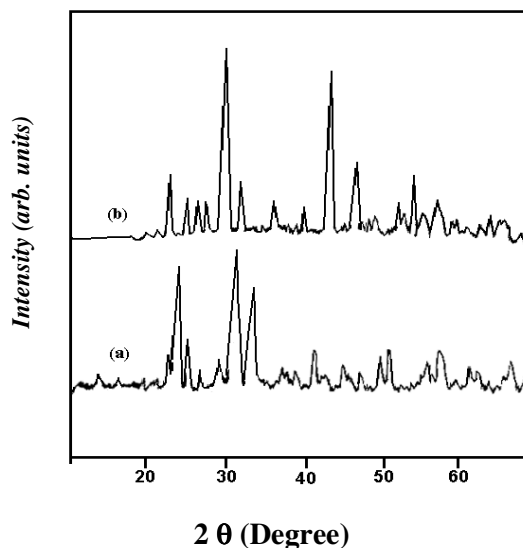


Figure-2: The X-ray diffraction patterns of the prepared ultramarine blue and violet containing:

- a) Sulfur as sulfur precursor.  
b) Sulfur as sulfur precursor and  $\text{NH}_4\text{Cl}$

The IR absorption spectral bands of ultramarine samples appear in the medium  $535\text{ cm}^{-1}$  and  $1123 - 1129\text{ cm}^{-1}$  region<sup>24</sup> (Fig. 3. and Table 3). It can easily be seen that, the IR spectra modes in this region are believed to originate from  $\text{S}^{-3}$  &  $\text{S}^{-2}$  in a sodium aluminosilicate matrix  $\text{Na}_8[\text{Al}_6\text{Si}_6\text{O}_{24}]\text{Sn}^{18}$ . It has been found that the IR absorption bands at  $1123 - 1125\text{ cm}^{-1}$  suffers shift to shorter wave number (red shift) in ultramarine samples containing S element to ultramarine samples containing S and  $\text{Na}_2\text{SO}_3$  as sulfur precursor associated with increase in the intensity of the blue colour of the synthetic ultramarine<sup>19</sup>. The IR absorption spectral band at  $624\text{ cm}^{-1}$  is due to Si-O stretching vibration<sup>20</sup>. The IR absorption bands appearing at  $\cong 3428\text{ cm}^{-1}$  and  $1627\text{ cm}^{-1}$  are characteristic for water of crystallinity.

The ultramarine samples were subjected to UV/visible absorption spectral measurements using

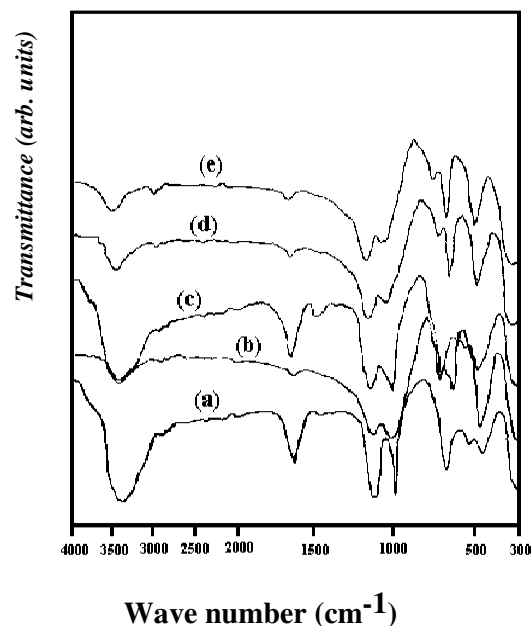


Figure-3: The infrared absorption spectra of the prepared ultramarine samples containing:

- a) Sulfur element                      b)  $\text{Na}_2\text{S}$   
c)  $\text{Na}_2\text{S}_2\text{O}_3$                               d)  $\text{Na}_2\text{SO}_3$   
e) Sulfur and  $\text{Na}_2\text{SO}_3$

glycerin suspension<sup>15</sup> and they were comparable to those of commercial ultramarine (produced by Reckit's colours of polifarb). The estimation was verified by electronic spectral assignments. The correlation between the absorbance measured for the samples and the wave number. Fig. 4 indicates the maximum intensity of the band at  $\sim 610\text{ nm}$  for the sample prepared with poly sulfide (5,6). The highest intensity of blue colour of the above two samples could result from feasible formation of  $\text{S}_3^-$  radicals from  $\text{S}_3$  anion<sup>21</sup>. The maximum of this absorption peak are slightly shifted towards higher frequency blue shift ( $604\text{ nm} - 606\text{ nm}$ ) compared to that of commercial ultramarine  $610\text{ nm}$ . There is other band notable in the spectral at  $\sim 370\text{ nm}$ . This band is assigned to  $\text{S}_2$  species<sup>21</sup>. The absorbance of this band is considerably higher for polysulfides than for sulfide or elemental sulfur. The intensity of this peak does not depend considerably on sulfur number<sup>21</sup>. The band appears at  $\sim 610\text{ nm}$  was shifted to lower frequency for nearly prepared samples (1), (2), (3), (4), (5), (6), (7). We deduced that the maximum intensity of this peak depends considerably on the calcination time as well as on the sulfur number (or sulfur precursor). It was

noted that high firing temperature during ultramarine synthesis led to deep blue colouration (see fig. 4). There is also another electronic band appearing at  $\sim 238$  nm the absorbance of this band increase with colour intensity and sulfur precursor increases. It has been found that the absorbance of the band at 604 nm decreases as sulfur precursor decrease and also by the addition of ammonium chloride to either prepared samples or to its starting mixtures (fig. 4).

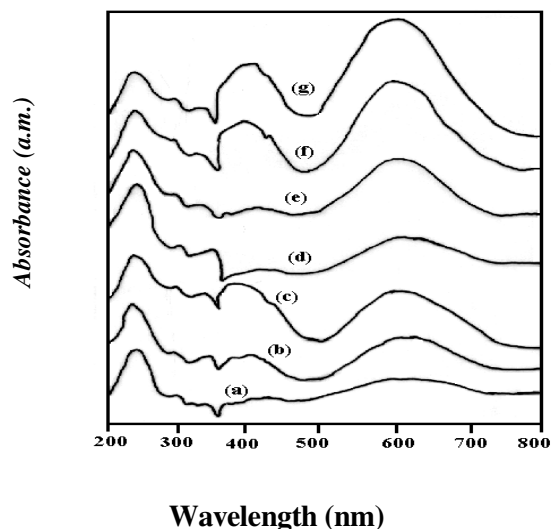


Figure-4: Electronic absorption spectra of the prepared ultramarine samples containing:

- a) Sulfur element    b) Sulfur element and  $\text{NH}_4\text{Cl}$   
 c)  $\text{Na}_2\text{S}$                       d)  $\text{Na}_2\text{S}_2\text{O}_3$   
 e) Contain  $\text{Na}_2\text{SO}_3$         f) Sulfur and  $\text{Na}_2\text{SO}_3$   
 g) Sulfur and  $\text{Na}_2\text{SO}_3$  (fired for 10 hr)

Figs. 5 and 6 represent the TGA and DTA curves of ultramarine samples containing sulfur as sulfur precursor, the two endothermic peaks at  $95.13^\circ\text{C}$  and  $772.93^\circ\text{C}$  and three exothermic peaks with maximum at  $170.23^\circ\text{C}$ ,  $245.42^\circ\text{C}$  and  $353.95^\circ\text{C}$ . The first endothermic peak at  $95.13^\circ\text{C}$  which is accompanied by 1.84% weight loss (see DTA curve fig.5 is associated to dehydration of humidity water content<sup>22</sup> and the second broad endothermic peak at  $772.93^\circ\text{C}$  which is accompanied by 1.10% weight loss (see DTA curve fig. 6), is due to  $\text{CO}_2$  evolution and oxygen uptake (oxidation) during the formation of ultramarine blue. The first exothermic peak at  $170.23^\circ\text{C}$  is accompanied by 5.44% weight gain (see TGA curve) is assigned to the first step of

partial oxidation of charcoal and evolving  $\text{CO}/\text{CO}_2$  during the formation reaction. The two exothermic peaks at  $245.42^\circ\text{C}$  and  $353.95^\circ\text{C}$  which are accompanied by 1.95% and 1.68% weight gain (see TGA curve fig. 5) are assigned to the second step in the partial oxidation of charcoal and evolving  $\text{CO}/\text{CO}_2$  during the formation reaction. The weight loss caused by evolving  $\text{SO}_2$  is almost negligible<sup>15</sup>. Thus, result of TGA and DTA for these faint blue ultramarine samples are in full agreement and support one another.

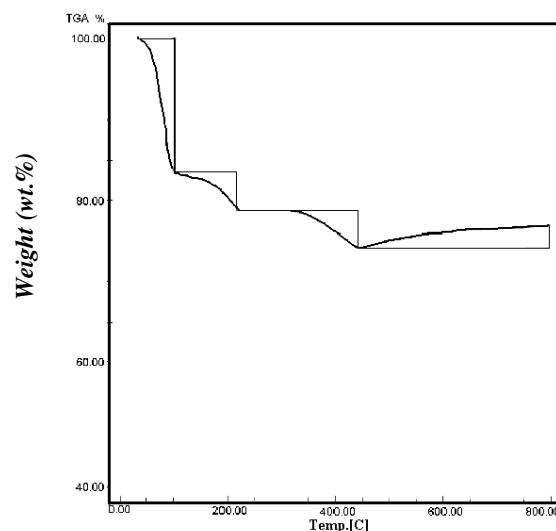
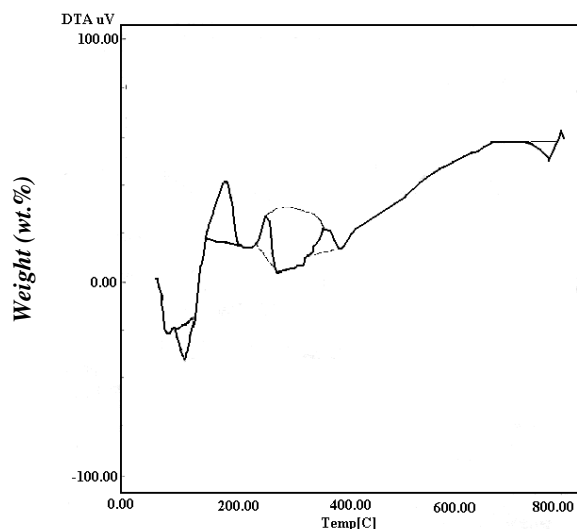


Figure-5: The thermogravimetric analysis (TGA) of ultramarine sample containing sulfur element

For the sample with sodium sulfite ( $\text{Na}_2\text{SO}_3$ ) as sulfur precursor fig. 7 and 8 represents the TGA and DTA curves of the sample. Two endothermic peaks are observed with maxima at  $102.65^\circ\text{C}$  and  $442^\circ\text{C}$ . Other three exothermic peaks are observed with maximum at  $197.02^\circ\text{C}$ ,  $242.36^\circ\text{C}$  and  $360^\circ\text{C}$ . The first endothermic peak at  $102.62^\circ\text{C}$  which is accompanied by -5.08% weight losses (see TGA curve fig. 9) is associated to the dehydration of humidity  $\text{H}_2\text{O}$  content<sup>22</sup>. The second endothermic peak at  $440^\circ\text{C}$  (see DTA curve fig. 8) is assigned to oxygen uptake (oxidation) and  $\text{CO}_2$  evolution during the formation of ultramarine.

The first exothermic peak at  $197.02^\circ\text{C}$  which is accompanied by - 5.08% weight loss (see DTA curve fig.8) is assigned to the first step in the



**Figure-6: The differential thermal analysis (DTA) of ultramarine sample containing sulfur element**

partial oxidation of charcoal and evolving CO/CO<sub>2</sub>. The two stepwise exothermic peaks at 242.38°C and  $\cong$  360°C which is accompanied by 1.75% weight gain (see DTA curve Fig. 8) are assigned to the second step in the partial oxidation of charcoal and evolving of CO/CO<sub>2</sub>. The weight loss caused by evolved SO<sub>2</sub> is negligible<sup>15</sup>. Thus, results of TGA and DTA are in full agreement for these blue ultramarine samples and support one another.

Figures: 9 and 10 display the ESR spectra of blue ultramarine (containing S and Na<sub>2</sub>SO<sub>3</sub> fired at 750°C for 3 h) and deep blue ultramarine (containing S and Na<sub>2</sub>SO<sub>3</sub> fired at 750°C for 10 hr), respectively. Their calculated g values are found to be (g = 1.93) for the blue ultramarine and (g = 1.94) for the deep blue ultramarine as shown in Figs. (9,10). It was established that the presence of S<sub>3</sub><sup>-</sup> radicals were confirmed by ESR<sup>15</sup> and their ESR signal anisotropy can result from the extra cages S<sub>3</sub><sup>-</sup> radicals<sup>15</sup>. In our investigated ultramarine sample, ESR data indicated further anisotropy comparing with earlier investigators<sup>15</sup>. This explains the more colour deepening in our deep blue ultramarine sample regarding our mode of synthesis and raw material included to modify the product for industry.

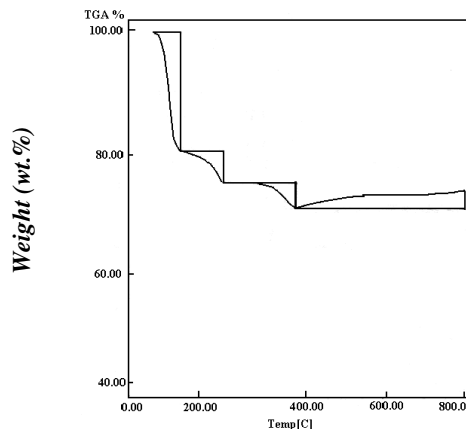


**Figure-7: The thermogravimetric analysis (TGA) of ultramarine sample containing Na<sub>2</sub>SO<sub>3</sub>**

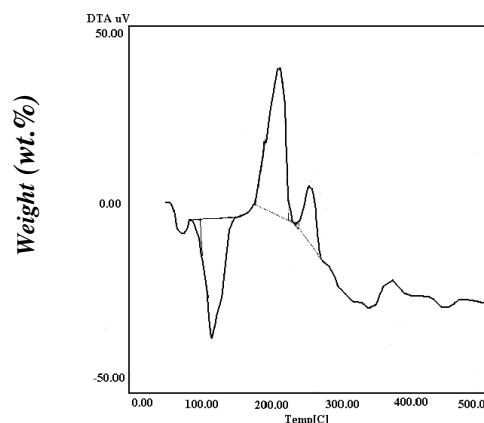


**Figure-8: The differential thermal analysis (DTA) of ultramarine sample containing Na<sub>2</sub>SO<sub>3</sub>**

Figures: 11 and 12 display variation of DC-electrical conductivity (log  $\sigma$ ) as a function of reciprocal of the absolute temperature (1000/T)K<sup>-1</sup> for synthesized ultramarine. It can easily be shown that, the material investigated is semiconductor because of the positive slope as shown in figures 11 and 12. In certain region of the curve, ultramarine sample shows metallic conduction in addition to its metallic semiconducting character. The ultramarine sample (containing sulfur element as sulfur precursor and fired at 750°C for 4 h), is a semiconductor in the range 318 – 673 K. In the range 318-498 K the ultramarine sample behaves as extrinsic semiconductor so the 498 K corresponds to transition from extrinsic to intrinsic semiconduction mechanism.

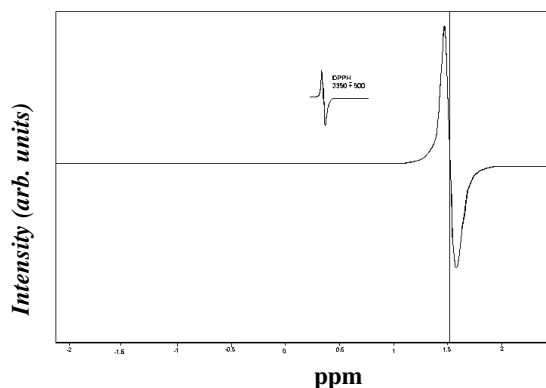


**Figure-9: ESR Spectra at room temperature for ultramarine sample containing sulfur element**

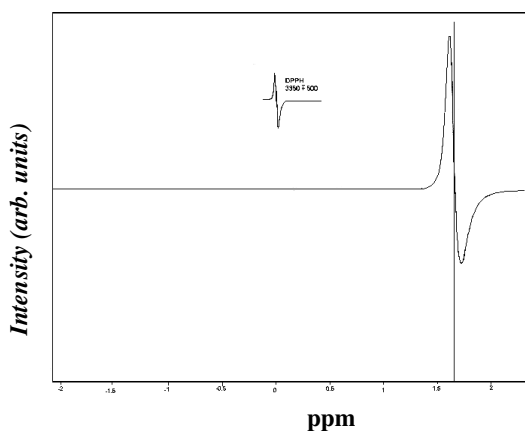


**Figure-10: ESR Spectra at room temperature for ultramarine sample containing sulfur element**

Applying the Arrhenius plot equation [23]

$$\sigma = \sigma_0 e^{-\Delta E/KT}$$

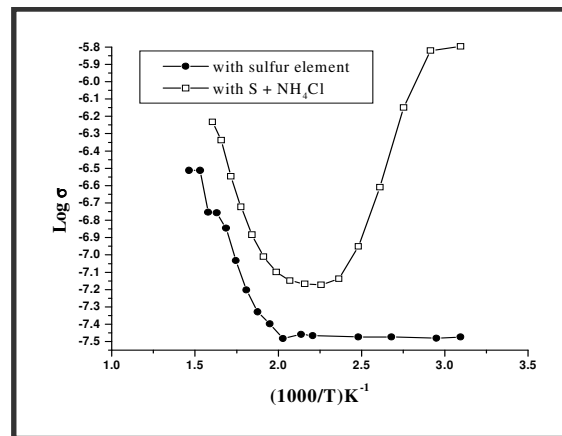
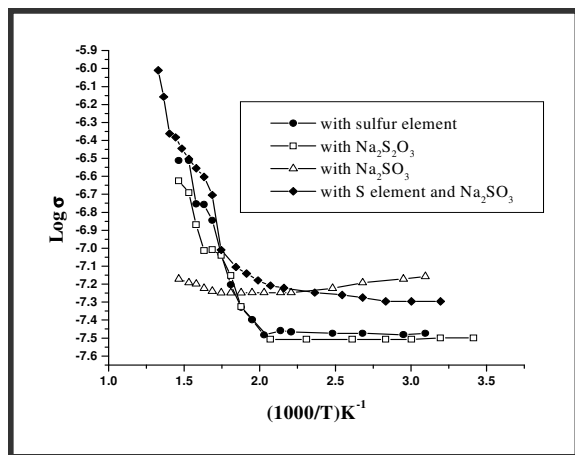
Where  $\sigma$  is the electrical conductivity at temperature  $T$ ,  $\sigma_0$  is the pre-exponential factor,  $K$  is the Boltzmann's constant and  $T$  is the absolute temperature. The intrinsic activation energy for electric conduction is calculated to be 0.041 eV in the temperature range 498 – 673 K. Thus the corresponding energy gap is evaluated to be 0.082 eV. The ultramarine sample (3) behaves as a semiconductor in the range 293 – 688 K, on the same proceeding rule, at the temperature range 298 – 473 K investigated; this ultramarine sample (3) behaves as extrinsic semiconductor. The 473 K is the transition temperature from extrinsic semiconductor to intrinsic semiconductor. In the range 473 – 673 K, there is intrinsic semiconduction. After applying Arrhenius plot, the activation energy for electric conduction is calculated to be 0.816 eV in the temperature range

investigated. It is generally accepted that the presence of  $S_3^-$  is a prerequisite step for semiconductivity in prepared samples and this formation of radical cause current flow. For ultramarine sample (5), the material is semiconductor in the temperature range 398 – 838 K. In the range 398 – 563 K this ultramarine sample (4) behaves as intrinsic semiconductor while in the temperature range 563 – 838 K behaves as extrinsic semiconductor. The 563 K being the transition temperature from extrinsic to intrinsic semiconductor. Applying the Arrhenius plot, the activation energy for electric conduction is calculated to be 0.044 eV in the temperature range 563 – 838 K. The induced metallic conduction mechanism in the extrinsic range (low temperature) is due to thermal decomposition. Our prepared ultramarine sample (6) is semiconductor in the range 313 – 753 K. In the range 313 – 463 K ultramarine sample (6) behaves as extrinsic semiconductor with a transition temperature of 463 K from extrinsic to intrinsic semiconductor. Applying the Arrhenius plot, the activation energy for electric conduction is calculated to be 0.099 eV in the temperature range 463 – 753 K. For our prepared ultramarine violet sample (7), there are two conduction mechanism appear to operate as follows: The first being the metallic conduction mechanism in the extrinsic range (318 – 403 K) may due to the presence of  $NH_4$  at low temperature and this greatly enhance some rearrangements of the electronic band structure of our prepared ultramarine violet sample. This inflection in the conductivity temperature (fig. 11) is interpreted on the basis of the occurrence of phase changes as detected from the DTA curve indicating its endothermity accompanied with colour faddening. The second being the semiconducting mechanism in the temperature range 408 – 623 K, After applying Arrhenius plot, the activation energy for electric conduction is calculated to be 0.073 eV in the temperature range 453 – 623 K, thus the corresponding energy gap is calculated to be 0.146 eV.

From Table (3) it can easily be seen that the activation energy for intrinsic semiconduction and hence the corresponding  $E_g$  decrease in the direction from sodium thiosulfate  $Na_2S_2O_3$



containing ultramarine (0.041 eV). Thus the semiconductivity is modified by sulfur addition, then  $\text{Na}_2\text{SO}_3$ ,  $\text{NH}_4\text{Cl} + \text{S}$ ,  $\text{Na}_2\text{SO}_3 + \text{S}$  and further by  $\text{Na}_2\text{S}_2\text{O}_3$ .



Figuer-12: The variation of DC-electrical conductivity ( $\log\sigma$ ) versus reciprocal of absolute temperature  $(1000/T) \text{ K}^{-1}$  for ultramarine samples

97

Table-1: The effect of the sulfur precursor on the structure and the colour of the prepared ultramarines

Sample	$\text{S}^{3-}$ precursor	Colour	Calcination temperature	Time (hrs)	Structure after calcination
Ultramarine blue	S	Light blue	400°C	2	Unknown
	$\text{S}_2\text{O}_3$	Light blue	750°C	4	Sodalite
	$\text{S}_2\text{O}_3$	Blue	750°C	6	Sodalite
	$\text{SO}_3$	Blue	750°C	3	Sodalite
	$\text{SO}_3$	Blue	750°C	6	Sodalite
	$\text{Na}_2\text{SO}_3 + \text{S}$	Blue	750°C	4	Sodalite
	$\text{Na}_2\text{SO}_3 + \text{S}$	Deep blue	750°C	4 then 6	Sodalite
	$\text{Na}_2\text{S}$	Gray	750°C	6	Sodalite
Ultramarine violet.	$\text{Na}_2\text{SO}_3 + \text{S} + \text{NH}_4\text{Cl}$	Violet	750°C	4	Sodalite

**Table-2: Characterization and band assignment of the infrared absorption bands (cm<sup>-1</sup>) of ultramarine samples (1,2,4,5,6)**

Ultramarine samples					Band assignment of the most
(1)	(2)	(4)	(5)	(6)	characteristic absorption bands
3427 <sup>b</sup>	342 <sup>m</sup>	3419 <sup>b</sup>	3428 <sup>m</sup>	3429 <sup>m</sup>	Asymmetric and symmetric stretching vibration of H <sub>2</sub> O.
1623 <sup>s</sup>	1614 <sup>v.w</sup>	1633 <sup>s</sup>	1628 <sup>w</sup>	1627 <sup>v.w</sup>	Bending vibration mode of H <sub>2</sub> O.
1127 <sup>s</sup>	1123 <sup>m</sup>	1129 <sup>m</sup>	1123 <sup>m</sup>	1126 <sup>m</sup>	S <sub>3</sub> <sup>-</sup> & S <sub>2</sub> <sup>-</sup> in a sodium alumino-silicate matrix
1001 <sup>v.s</sup>	1012 <sup>m</sup>	1002 <sup>s</sup>	1025 <sup>w</sup>	1026 <sup>w</sup>	Associated with the Si-O stretching vibration.
534 <sup>w</sup>		536 <sup>w</sup>			S <sub>3</sub> <sup>-</sup> & S <sub>2</sub> <sup>-</sup> in a sodium alumino-silicate matrix.
	623 <sup>m</sup>		624 <sup>v.b</sup>	624 <sup>v.s</sup>	Silica spectrum Na-O stretching on vibration and also due to SiO stretching vibration

97

**Table-3: The transport data for the prepared ultramarine blue sample**

Ultramarine No.	Composition	Intrinsic Activation energy (Δ E <sub>o</sub> eV)	Energy gap (E <sub>g</sub> eV)
(1)	Kaolin + Na <sub>2</sub> CO <sub>3</sub> + S + Charcoal	0.041	0.082
(2)	Kaolin + Na <sub>2</sub> CO <sub>3</sub> + Na <sub>2</sub> S <sub>2</sub> O <sub>3</sub> + Charcoal	0.816	1.632
(4)	Kaolin + Na <sub>2</sub> CO <sub>3</sub> + Na <sub>2</sub> SO <sub>3</sub> + Charcoal	0.0435	0.087
(6)	Kaolin + Na <sub>2</sub> CO <sub>3</sub> + S + Na <sub>2</sub> SO <sub>3</sub> + Charcoal	0.099	0.198
(7)	Kaolin + Na <sub>2</sub> CO <sub>3</sub> + Na <sub>2</sub> SO <sub>3</sub> + S Charcoal + NH <sub>4</sub> Cl	0.073	0.146

**References**

- Kowalak S., Stawinski K., Walowska R., and Zadrazona E., Zeolite Callog, 3<sup>rd</sup> (Pub. 1998), 113, (1997)
- Gobeltz N., Demontier A., Leieur J., and Duheyon C., *J. Chem. Soc. Faraday Trans.*, **94(15)**, 2257 (1998)
- Kowalak S., Pol. Pt **172**, 362 (Cl. Co 9 Cl/32), (1997)
- Tae Y., Yoon C.Y., and Woong H.S., Shigen to Sozai, **114(2)**, 106 (1998)
- Kowalak S., Pol. Pt. 171, 246 (Cl. CO9C1/32) (Pol) (1997).
- K. Leschewski and H.Moller, *J. Appl. Phys.*, **65**, 250 (1932).
- Jaeger F.M., *Bull J., Ceram. Soc.*, **53**, 183, (1930)
- Hoffmann J., anorg Z. and Allgem, *J. Chem., Soc.*, 189-91 (1930)
- Kook H. S., Tae Y. Y., Yoon C. Y., and Woong, Han'guk H. S., Chaelyo Hakhoechi, **7(10)**, 863 (1997)

10. Gobeltz N., Demortier A., Lelieur J. P. and Duhayon C., *J. Chem. Soc., Faraday Tran.*, **94(5)**, 677 (1998)
11. Balkus K. J., and Kowlak S., U. S. Patent S, **167**, 942 (1992)
12. Stoky G. D., Srdanov Harrison W.T.A., Gier T.E., Keder N.L., Moran K.L., Haug K., and Metiu H.I., *J. ACS Symposium series* **499**, 294 (1992)
13. Kowalak S., Pulish Patent Appl., P-302065.
14. Kowalak S., Stawinski K., Walawska R., and Zadro E., *J. Chemia.*, 16, 212, (1999)
15. Kowalak S., Strozyk M., Pawlowska M., Miluska M., and Kania J., *Studies in Surface science and Catalysis*, **105**, Elsevier Science BV (1997)
16. Seel F., *J. Chemia*, 5, 69 (1994)
17. Kowalak S., Polish Patent ppl., P – 301761 167 (1992)
18. Wieckowski A.B., Proc. Ramis-79, Poznan, 265 (1979)
19. Karranov J. C., *J. Inorganic Chem.*, 5, 3808 (1986)
20. Bouhet C., and Lafont R., *J. Acad. Sci.*, 226, 1263, (1948)
21. Kera Y., *J. Bull. Chem. Soc. Jpn.* **57**, 1478 (1984)
22. Zurkova L., Sucha V., *J. Thermochim. Acta.*, **98**, 255, (1986)
23. Abou-Sekkina M.M., *J. Phys. Stat. Sol.*, (a) **146**, 51 (1994)